Thermal Analysis of the Sinus Filter and Verification

Jan Kořínek[1]

[1] *Jan Perner Transport Faculty, University of Pardubice, Studentská 95, 532 10 Pardubice 2, Czech Republic*

Abstract

This article discuss the relationship between the power losses of a sinus filter and their influence to distribution of temperature field inside, on the surface and in the surroundings of the sinus filter under load. It is possible to find here description of three-dimensional CFD analyses creation for case of heat transfer by natural convection into surroundings, comparison of various variants and evaluation of the results. Description of validation methodic for CFD analysis is mentioned as well with final evaluation and comparison between experimentally gained data and simulated results.

Keywords: STČ; choke; sinus filter; Ansys; heat transfer; FEA; magnetism; natural convection; CFD

1. Introduction

The sinus filter is used for ensuring the device electromagnetic compatibility. For a description of heat transfer relations in magnetic field and in winding it was created 3D thermal model of the sinus filter choke.
In case of the wound parts design, magnetic circuit is influenced by thickness of the used material and high frequency part of the current, which contains wide spectrum of harmonics. In calculation, it is necessary to count with basics harmonics and determine their values with consideration of other harmonic losses. Next factor is achieved for warming of the device. This warming causes rising of the sinus filter losses [1].

From reasons above, it was realized an experimental measurement for validation of losses and for validation of the CFD simulation of the temperature distribution through the sinus filter choke. It was also measured current, which goes through the sinus filter. Thanks to that, it is possible to divide losses in part of the core and part of the winding. Values from these parts are used as boundary conditions for the CFD simulation of the temperature distribution. Measurement of achieved temperature values on a physical sample of the sinus filter is then used for overall comparison with the CFD simulation.

2. Sinus filter wiring description

Sinus filter is designed for nominal current 16 A, switching frequency from 2 kHz and for short-time overload 1.5 times. Output voltage is from 0 to 500 V. Supply wire from a low voltage net 3x230/400V was connected into the three phases commutating choke. Commutating choke was plugged into the frequency converter and on the output clamps, the sinus filter was connected. Measurement were carried out on the sinus filer however simulation was performed for the geometry of the sinus filter choke. Behind the sinus filter a constant load was plugged in. Sinus filter input was connected to the output inverter of the frequency converter Siemens Masterdrives of the power 11 kW. Frequency converter built on his output an associated pulse width modulation voltage PWM pulsing with 4 kHz frequency. Sinus filter output was connected to the electric motor. This voltage was filtrated with the bottom gate LC type under the 1 kHz limit. Behind this bottom gate (sinus filter), the voltage was brought the constant load.

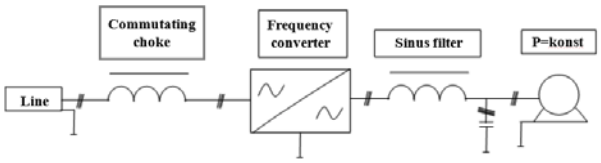

Fig. 1. *Schematic wiring description of sinus filter.*

3. Thermal analysis methodic

Three variants of different thermal analysis approach were performed.

First variant consider geometrically simplified CAD data of the sinus filter choke model with characteristic dimensions based on product specification. Computation task, its settings, mesh creation, definition of boundary conditions and final post processing were conducted with the Ansys Transient Thermal software. Simulation considers transient case, therefore the temperature change process can be observed in core, winding frame, windings and the clamping construction.

Second variant consider same CAD data and material characteristics. Difference can be found in approach how calculated heat transfer from filter into surroundings. In first variant is considered manual computation of heat transfer coefficient and set up as one of boundary conditions, however in second variant is numerically calculated by software as a one of the results. Therefore, temperature distribution from second variant is solved by Ansys Fluent module.

Third variant uses same computational approach of heat transfer coefficient as previous variant two. In this case, major difference is obtained by more complex geometry from CAD data. There are included additional parts like capacitors, screws, mountings. Coils, mounting

* Kontakt na autora: korinek.j@gmail.com

brackets and bobbins are remodeled into significant increase of detail. Whole case is solved again in Ansys Fluent. Due to added capacitor parts, we can use term "Sinus Filter" compared to "Sinus Filter Choke" in first two cases. [6]

3.1. Geometry and materials of the model

The filter core consists of isotropic cold rolled metal sheets. Their count defines the final core width. Since the metal sheets are in close contact, for the calculation purposes it is considered the monolithic core model keeping the characteristic dimensions according to Waasner DIN EN 10106, EI 175/175 with material characteristic M330-50A. For the calculation purposes, the similar assumption was considered as well as in the case of the copper winding. The winding represents a monolithic solid and characteristic dimensions related to the sinus filter product specification. To the winding frame the material characteristics for Pocan B4239 are assigned. For the model mesh optimization of variant I and II was not considered a ribbing on the horizontal area of the frame. See full list of material properties assigned into each component in Tab.1. [6]

Tab 1. *Material properties.*

Var. usage	Part	Density ($kg \cdot m^{-3}$)	Specific Heat ($J \cdot kg^{-1} \cdot K^{-1}$)	Thermal Conductivity ($W \cdot m^{-1} \cdot K^{-1}$)
I,II,III	Core	7850	490	60,5
I,II,III	Bobbin	1500	1040	0,25
I,II,III	Coil	8933	386	400
III	Mountings	8933	386	400
III	Capacitor	1005	1765	0,19
III	Screw insulation	1500	1040	0,25
I,II,III	Steel parts	8030	502,5	16,3
III	Copper parts	8978	381	387,6

Complete 3D models for variants I, II and III are represented in Fig. 2, 3 and 4.

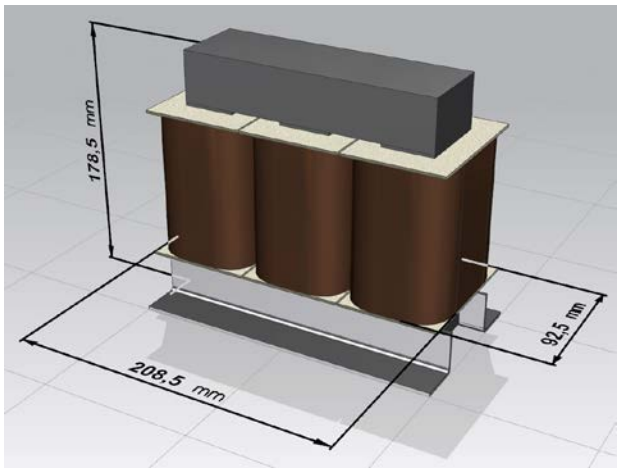

Fig. 2. *CAD model of sinus filter choke (variant I, II).*

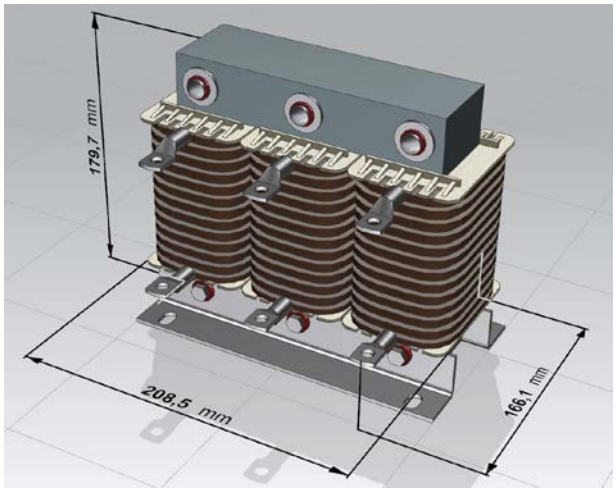

Fig. 3. *Detailed CAD model of sinus filter (variant III) – front.*

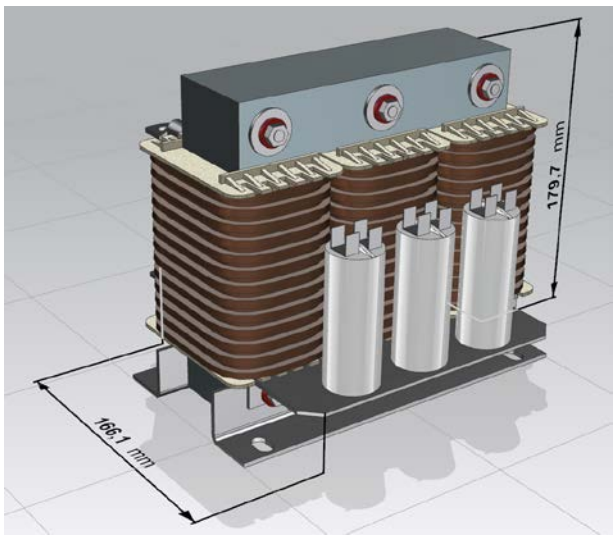

Fig. 4. *Detailed CAD model of sinus filter (variant III) – rear.*

3.2. Mesh properties

In case of variant I, was for reaching the lowest possible calculation time placed emphasis on optimization of element shapes, which build the whole model mesh. It contains only geometry from CAD data without usage of symmetry resemblance. Approximately 85 % of the mesh consists of hexahedral type elements.
Mesh for variant II and III contains surroundings computational domain of air (5m x 5m x 6m) as well. Most of elements are polyhedral type. Symmetry resemblance in ZY plain was utilized to decrease solution time.

3.3. Initial and boundary conditions, solver settings

3.3.1. Variant I settings

One of parameters entering into the calculation is the initial temperature. Due to the fact that during the experimental validation the environment temperature of the air was 15 °C, the same temperature was considered for the simulation. The final temperature settling time was set on 80 000 s.

Boundary condition of the heat flow was globally applied on the core and sinus filter winding. Manufacturer intention was to find out, for how long is possible to overload the sinus filter of 1.5 times of the nominal alternate current. Based on that losses on the core was 17.2 W/winding. Losses on the stand alone winding are 15.9 W. These values are crucial for heat distribution across whole geometry and has to be taken in account. Both of them were calculated and provided by manufacturer.

From the convectional heat transfer point of view, it is critical to determine as close as possible the heat transfer coefficient. Calculation of the heat transfer coefficient is dependent on character of the fluid flow, which is close to the sinus filter walls. It is also dependent on whole geometry of the sinus filter. For discussed simulation was calculated 13 heat transfer coefficients as boundary conditions in range from 5 to 30 $W \cdot m^{-2} \cdot K^{-1}$. These values were constantly modified during simulation with temperature influence. In flow for actual fluid it is then necessary to consider kinematic and dynamic viscosity, heat conductivity, volume expansion and also specific heat capacities. Air is considered as an ambient medium and its properties as temperature depended. In consequence of this fact we get for each determining temperature other values of Grashof, Prandtl, Rayleigh and Nusselt numbers. The resulting heat transfer coefficient – see (1), where Nu is Nusselt number, L is characteristic dimension and k correspond to thermal conductivity which is related to certain geometrical area is thus continuously changing till reaching the established temperature [2] [3].

Due to very comprehensive problematics related to hear transfer coefficient, the detailed discussion about calculation is over the scope of the article.

$$h = \frac{Nu \cdot k}{L} \qquad (1)$$

where

$Nu = Nusselt\ number\ (-)$
$L = characteristic\ dimension\ (m)$
$k = conductivity\ (W \cdot m^{-1} \cdot K^{-1})$

3.3.2. Variant II and III settings

With respect to different computational approach than in case of variant I, it´s not necessary to compute heat transfer coefficients separately to include them as one of the inputs of boundary conditions.

Whole case is the solved by pressure-based solver with consideration of gravity influence as pseudo-transient solution. Advantage of this approach lie in automatic calculation of solid/fluid pseudo time step. Due to that, length scale for solid and for fluid are calculated separately which cause to reach of convergence more quickly. Transient calculation in this case would need approximately 46 days of computer time to reach steady state. Pseudo transient approach take about 4 hours to reach steady state to maximal temperature.

Computational model include energy equation as well. This equation represent energy transfer due to conduction, species diffusion, and viscous dissipation, and volumetric heat sources. In solid regions, the energy transport equation has the following form – (2). [5]

$$\frac{\partial}{\partial t}(\rho h) + \nabla \cdot (\vec{v}\rho h) = \nabla \cdot (k \nabla \mathrm{T}) + S_h \qquad (2)$$

where

$t = time\ (s)$
$\rho = density\ (kg \cdot m^{-3})$
$h = sensible\ enthalpy$
$\vec{v} = velocity\ (m \cdot s^{-1})$
$k = conductivity\ (W/m^{-1} \cdot K^{-1})$
$T = temperature\ (°C)$
$S_h = volumetric\ heat\ source$

Determination of flow behavior was done by indication of Rayleigh number (3).

$$Ra = \frac{g\beta\Delta T L^3 \rho}{\mu\alpha} \qquad (3)$$

where

$g = gravitational\ acceleration\ (m \cdot s^{-2})$
$\beta = thermal\ expansion\ coeficient\ (K^{-1})$
$\mu = dynamic\ viscosity\ (Pa \cdot s)$
$\alpha = thermal\ difussivity\ (m^2 \cdot s^{-1})$

In this case, average value of Rayleigh number is up to 10^8. This indicates laminar character of the flow.

Boundary conditions of ambient temperature and power losses of sinus filter remain same as in variant I.

4. Verification temperature measurement

The sinus filter was placed in an area on the horizontal plate without forced flowing or actuation of further heat sources. Ambient temperature of air was 15 °C. So the character of flow around the walls corresponds with the free convention. Sinus filter was powered by alternating current frequency of 50 Hz with superimposed high-frequency component resulting from switching frequency of the frequency converter. Temperature measurement of the sinus filter loaded with the 23 A current has taken place using thermocouples and thermovision. There could be also taken in account usage of resistance method thanks to that is possible to find out the average thaw of windings. However, in our case was used thermovision which provided to us accurate temperature field distribution and not just average value. [6]

Thermocouple using principle of the direct temperature difference conversion in electric voltage is the class T with the maximum allowed usage temperature to 350 °C. It is produced from the combination of copper and constantan material. The measurement error is 0.75 % at the temperature above 0 °C. Thermocouples are connected with the auto-calibrating unit National Instruments® Ni PXI. This unit is used for digitization, archiving and for evaluation of the warming procedure. In total, it were used four thermocouples allocated at different measuring points – see Fig. 5. Based on sinus filter design and measurement options, thermocouples were placed as close as possible to places with highest expected temperature without any damage of sinus filter. Thermocouple No. 1 measures the temperature on the core surface. Thermocouple No. 2 is positioned under surface between the core and winding frame (place with highest expected temperature). Thermocouple No. 3 is inserted between windings and thermocouple No. 4 is in the opposite location on the bottom side of the core parallelly with the plate on which the sinus filter is placed. [6]

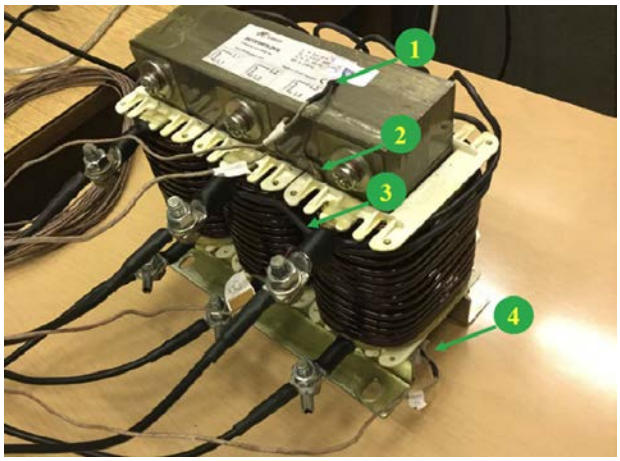

Fig. 5. *Sinus filter SKY3FSM16-2kHz with thermocouples [6].*

The second method of the temperature measurement was the screening of infrared radiation generated by the sinus filter surface. For this measurement the thermovision Fluke® Ti125 was used. For radiated infrared spectrum volume the fundamental factor is the surface temperature and emissivity of the material surface. Based on these recorded data the surface temperature is subsequently calculated by a thermocamera. Emissivity, which was set up in the device for the detection, was calibrated on the value 0.96 based on comparison with the measurement which was performed with the second sinus filter. The temperature of the second sinus filter is the ambient temperature. The temperature range for usage of the thermovision is from − 20 °C up to 350 °C with accuracy ±2 °C or 2 % based on fact which value is the bigger one. The temperature sensitivity of the detection is 0.1 °C if the temperature of the measured object is 30 °C according [4]. For the visualization of the recorded data, the color range with blue-red spectrum during the whole measurement was used. The reason for usage of this spectrum is better graphicness in comparison with the CFD simulation of the temperature allocation. [6]

5. Results evaluation

Comparison of achieved results will be divided into two separate sections based on it´s own comparable character. In first section are described results of thermocamera and thermocouples measurement in comparison with temperature filed from variant I simulation in time 5 hours of constant load.

In second section are compared steady state results of variant I, II and III.

5.1. Temperature field evaluation - 5 hours load

5.1.1. Thermocouple measurement

From the thermocouple measurement the warming characteristic was derived. The temperature monitoring from the start of loading took 5hours. Based on the measured data it was done the trend regression for smoothing.

For better orientation it were included the warming data from the simulation into the graph in Fig. 6 in order to enable the temperature trend comparison. Figure 6 demonstrates that the warming character from the simulation is approaching to the performed measurement.

The highest measured temperature after 5 hours was measured in the point No.2 with value 82.1 °C and thus in the location between upper part of the winding frame and core. 76.4 °C was identified on windings in the point No. 3. On the core surface in the point No. 1 it was found out 60 °C and in the point No. 4 the temperature was 60.6 °C. [6]

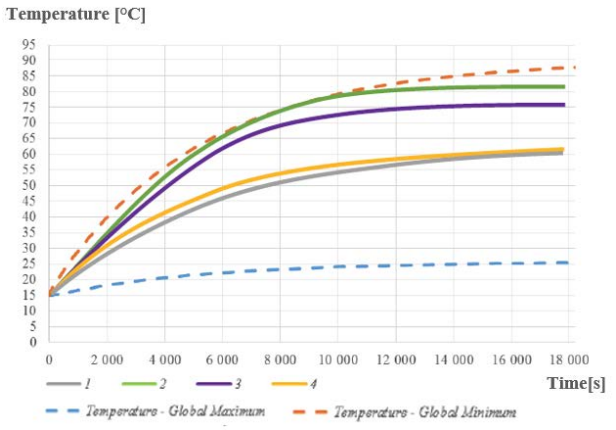

Fig. 6. *Settling of temperatures from points 1–4 measured by thermocouples[6].*

5.1.2. Thermovision measurement

On the below presented figure series it is always possible to see the temperature field recorded by the thermovision with the visualization of the temperature range and maximum temperatures reached in the concrete view. In addition, it will be introduced the assigned view of the 3D model from the simulation for comparison. Due to the fact that the real warming characteristic was measured for 5 hours, the compared views from the simulation are used as well from this time frame and not from the period of the stabilized state, that means derived for the time 18 000 s. Nevertheless, from Fig. 6 it is visible that the difference of the maximum temperature between this time frame and the stabilized state time is minimal. [6]

After deduction of the simulation data, the value corresponds with 2.5 °C.

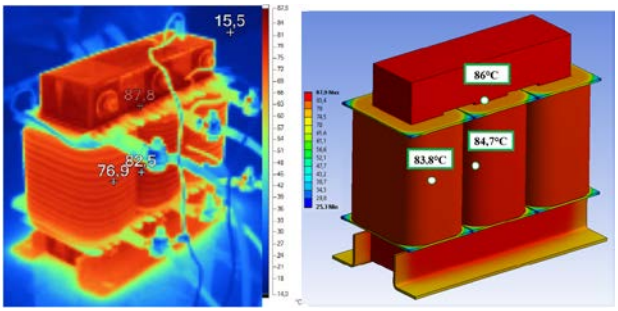

Fig. 7. *Comparison of temperature fields between thermovision and simulation in time of 5 hours.*

In Fig. 7 there are highlighted points for better orientation in the locations on the surface of the side and middle windings. Furthermore, there is shown the highest measured temperature in the actual snapshot at the value 87.8 °C. The same can be seen in the right side of the figure. It is visible that the differences here are commonly reaching 2.5 °C except the side winding where the temperature difference is up to 6.9 °C. From snapshots it can be derived that the real temperature field allocation on the middle winding corresponds with the simulation. [6]

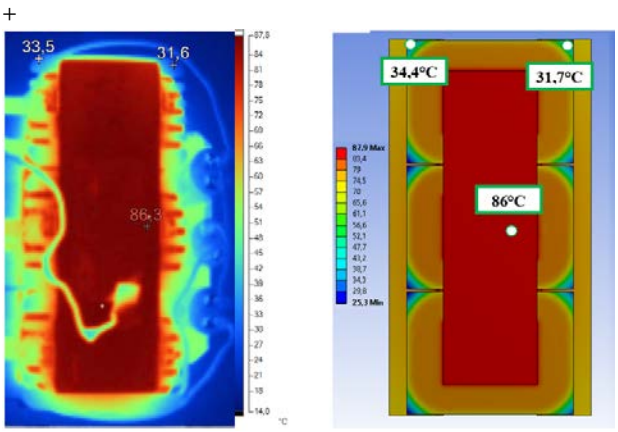

Fig. 8. *Comparison of temperature fields between thermovision and simulation in time of 5 hours – top view[6].*

In the locations at the winding frame edges the lowest temperature after stabilization based on the simulation was determinated. Verification is visible in Fig. 8. The measured temperatures in these edges were 31.6 °C and 33.5 °C. Highest difference against the simulation was in this case 1 °C. From the temperature allocation of the winding frame point of view, the calculation model corresponds in these locations with the reality. In Fig. 9 in the bottom area the measured temperature of the core near to the plate surface is visible. Compared to 85.6 °C from the simulation the measured temperature here is 83.4 °C. The temperature in the upper part from the core side differs not so much, only up to 1.1 °C. It was measured here 87.6 °C compared to 86.6 °C from the simulation. [6]

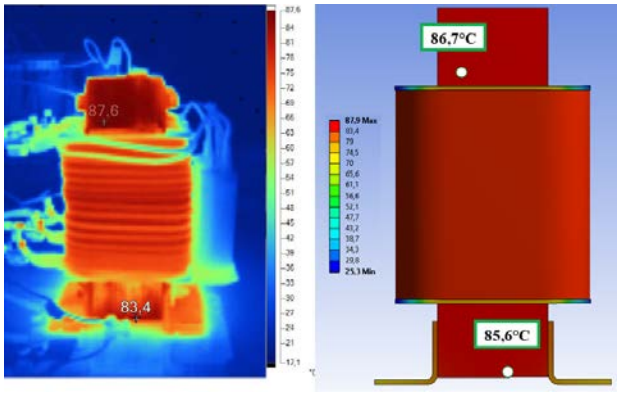

Fig. 9. *Comparison of temperature fields between thermovision and simulation in time of 5 hours – side view.*

In Fig. 10 the temperatures from measurement points 1−4 are listed. Maximum reached temperatures in these points are measured or calculated in the timestamp of 5 hours operation under load. The simulations are derived from the same locations with help of virtual probes. In case of infrared radiation, which was recorded by thermovision, the temperatures of the measurement locations are derived in figures with support of software for analysis and recording of the infrared figurers. [6]

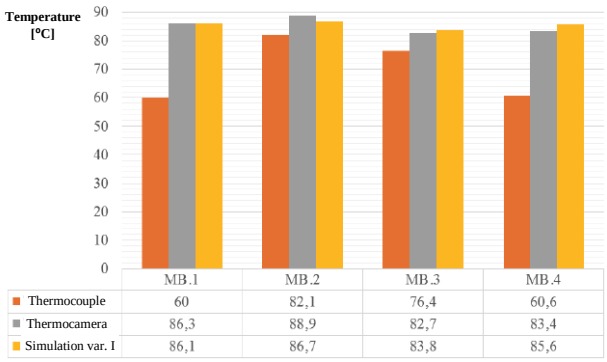

	MB.1	MB.2	MB.3	MB.4
Thermocouple	60	82,1	76,4	60,6
Thermocamera	86,3	88,9	82,7	83,4
Simulation var. I	86,1	86,7	83,8	85,6

Fig. 10. *Comparison of maximum temperatures by thermocouples, thermovision and variant I simulation[6].*

5.2. Temperature field evaluation – steady state

5.2.1. Variant I

From the performed variant I FEA simulation of the sinus filter choke it was calculated the 3D temperature distribution across inside and surface geometry, which is visualized in Fig. 11a. Color spectrum expresses the local temperature in °C. Calculation was executed as transient with the time step 1 s in the range from 0 to 80 000 s. Stabilized situation was reached after 154 iterations in the time 70 100 s. As a criterion for stabilized solution was set up an increment of 0.001°C. In the Fig. 11b can be also seen thermal gradient between location with highest temperature and surface of middle winding. Based on simulation, the gradient value is in this case 3,3°C. [6]

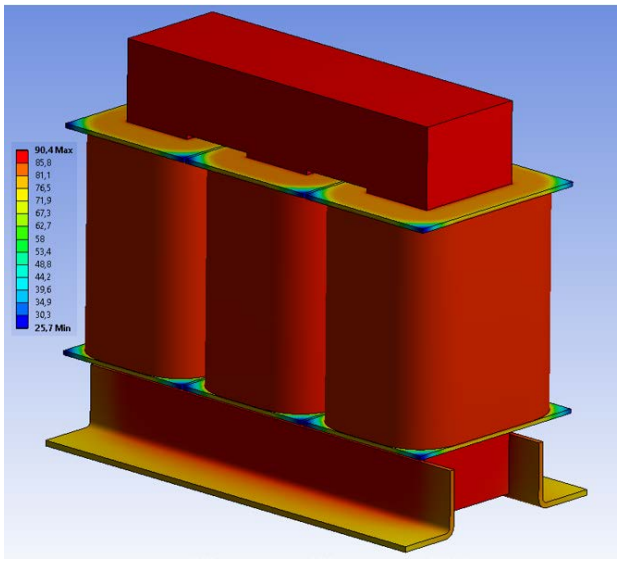

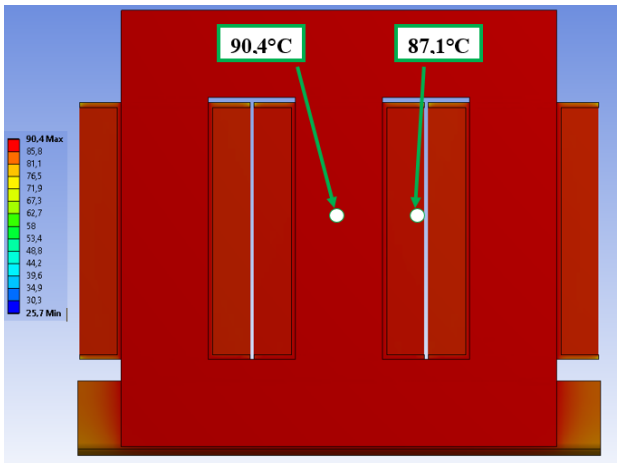

Fig. 11. *a) Stabilized 3D temperature field in time of 70 100 s. b) Longitudinal cross-section through sinus filter choke*

5.2.2. Variant II

Solution of variant II reached convergence after 1700 iterations. Temperature distribution looks similar to variant I, however there are still significant differences which can be found. Most important of them is achieved maximal temperature after the reach steady state. This temperature is 119,5°C and its located in the middle of the sinus filter choke - see Fig.12b. This fact correspond mostly with calculation of heat transfer coefficients from solid into ambient air. There is also relative difference between the center of the middle core temperature and temperature at the edge of the coil visible in section-cut. Temperature decreased only 0,1C. This is valid specifically for current section-cut through XZ. In other locations, decrease is significantly higher. Fig 12b shows surrounding temperature of the air near to sinus filter choke. This is advantage of current approach and can be used during planning of allocation into housings.

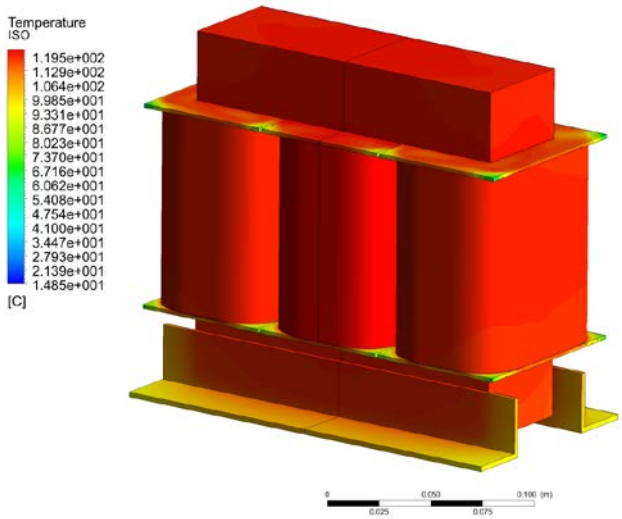

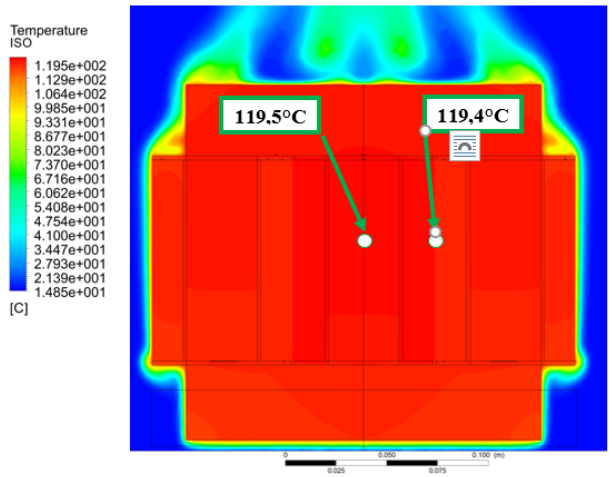

Fig. 12. *a) Stabilized 3D temperature field of variant II b) Longitudinal cross-section through sinus filter choke*

5.2.3. Variant III

Higher complexity of the geometry is taken into account regarding to variant III. Based on simulation results, this fact caused significant decrease of reached maximal temperature. After 1800 iterations temperature reached steady state at 102,9°C in the center of the core. Relative difference between the center of the middle core temperature and temperature at the edge of the coil in section-cut is 2,1°C.

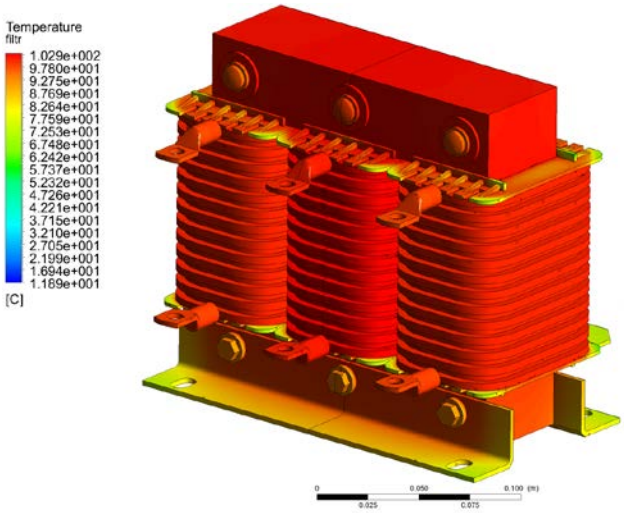

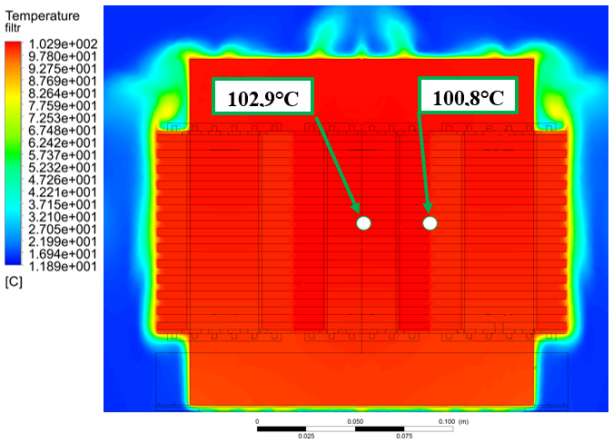

Fig. 13. *a) Stabilized 3D temperature field of variant III b) Longitudinal cross-section through sinus filter choke*

Fig. 13 show that temperature on mountings reach above 90°C. Heads of the screws has temperature in range from 80°C up to 90°C. Generally, most of the heat is located at the upper and central area of the sinus filter.

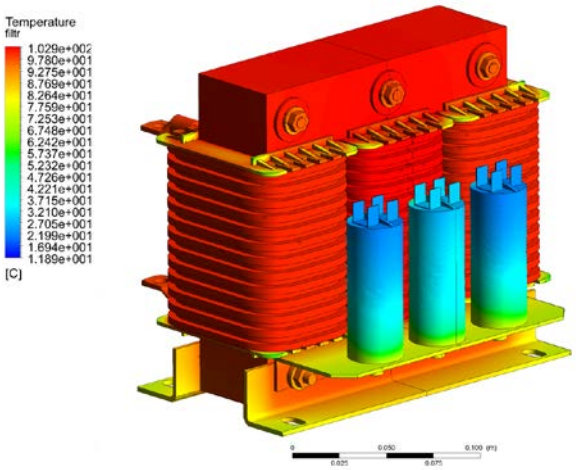

Fig. 14. *a) Stabilized 3D temperature field of variant III – rear view*

Temperature field across capacitors is shown at Fig. 14. Temperatures vary from bottom up to the top of the capacitor in range from 30°C up to 75°C. Generally, central capacitor is approximately about 10°C warmer than side capacitors.

5.2.4. Comparison of variants

In Fig. 15 the temperatures from measurement points 1−4 are listed. Maximum reached temperatures in these points are calculated steady state operation under load. The simulations are derived from the same locations with help of virtual probes.

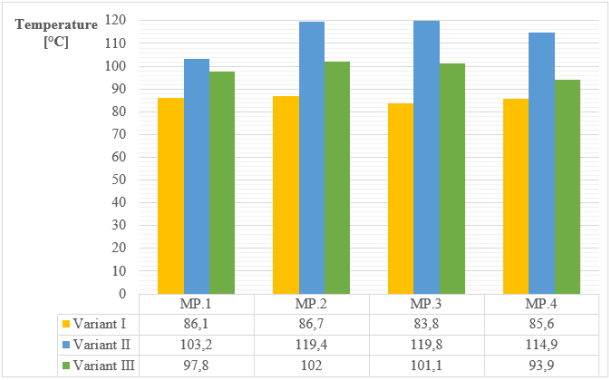

Fig. 15. *Comparison of maximum temperatures for steady state in point 1-4 of variants I-III*

Significant difference is between FEA simulation of variant I and CFD simulation of variant II. This show the impact of different approach of calculation of heat transfer coefficients. Prove of another fact is that higher complexity of geometry results in solution that is more accurate.

6. Conclusion

Based on comparison of the methods from chapter 5.1, the FEA simulation seems to be the most pessimistic one from the reached maximum point of view. It is possible to say that its results are most approaching in all measuring points to the values, which were measured by the thermovision. A considerable difference of temperatures measured by the thermocouple appeal in points 1 and 4, and thus on the upper and bottom horizontal sides of the core frame. Potential explanation could be found in the way of the thermocouple fixture, whose contact with the core surface may not be ideal. In general, the thermocouples seem to be the most optimistic solution from the reached temperature measurement point of view. To this statement contributes the fact that the thermocouple itself has its own level of the thermal conductivity. In the contact place thus comes to the heat transfer from the sinus filter material into the thermocouple. Therefore, the lower temperature is measured than the temperature, which is really on the sinus filter surface and its surrounding. As can be seen in Fig. 10, agreement between simulation and thermovision is satisfactory, therefore assumption of thermal gradient agreement is taken in account. Considering of surrounding temperature of 40°C in closed environment, sinus filter would be probably thermally overloaded in this case. Here is necessary to remind that main focus of the article is not sinus filter dimensioning for a specific application but to acquire data for validation of FEA simulation.

By the comparison of both thermovision and sinus filter choke 3D model views it is obvious that in some locations the temperature field differs more from the real allocation. In order to improve the accuracy of the temperature allocation this was optimized in the simulation through the improvement of the 3D geometry precision into higher details, e.g. implementation of winding frame ribbing, fastening contacts and condenser holders.

All of this leads into CFD simulation of variant III. At the real product of the sinus filter, the surface is due to the wire winding grooved. This fact has an influence on the flowing during free convention, when its character is changed due to the radial direction of the current through the winding grooves. The effect is a change of the heat transfer coefficient and thus the change of the resulting surface temperature. Implementation of more detailed winding geometry into the 3D model leads to the usage of correlation relationships, modified for the shape of the concrete geometry.

This fact is confirmed by presented results in chapter 5.2 where is possible to see that detailed geometry of variant III has generally lower temperatures than simplified geometry of variant II.

Further, the losses allocation in the winding has influence on the temperature differences in the single windings. In the 3D model in the boundary conditions, the same losses in every winding are considered. In the reality, the losses can be slightly different on the single windings. This would have the effect on the temperature difference increase between single windings as the results.

The mentioned facts above show the new potential that can be used for further concretization of the input parameters for the mathematical simulation model. In the near future, more geometrical details can thus be implemented into the actual model, application of the values of measured losses and thus reaching the change of the temperature field allocation.

Acknowledgment

This text was created with support of the project Studentská grantová soutěž SGSDFJP_2016001. Creation was also supported by company SKYBERGTECH s.r.o. which borrowed sinus filter and provided consultations during validation measurements.

References

[1] KRISHNAMOORTHY P. Electromagnetic and Heat Transfer Modeling of Microwave Heating in Domestic Ovens. Lincoln: University of Nebraska at Lincoln, May 2011.

[2] NOŽIČKA, J. Základy termomechaniky. Praha: Vydavatelství ČVUT, 2001. ISBN 80-01-02409-1.

[3] ŠESTÁK, J. a F. RIEGER. Přenos hybnosti, tepla a hmoty. Praha: Vydavatelství ČVUT, 1993. TA357.Š37 1993.

[4] FLUKE. fluke.com: Ti90, Ti95, Ti100, Ti105, Ti110, Ti125 TiR105, TiR110, TiR125 Performance Series Thermal Imagers [online]. © 2012 [cit. 2016]. Available on: http://www.fluke.com/fluke/czcs/support/manuals/default.htm

[5] ANSYS Inc. ANSYS Fluent Theory Guide. Canonsburg 2016: http://www.ansys.com.

[6] KOŘÍNEK, JAN. Transactions on electrical engineering. Validation of Sinus Filter Choke Temperature Model. Praha : ERGO NOMEN, o.p.s., K13114 FEE CTU in Prague, 2016. ISSN 1805-3386.